

ENVIRONMENTAL TOXINS

Models predict planned phosphorus load reduction will make Lake Erie more toxic

Ferdi L. Hellweger^{1*}, Robbie M. Martin², Falk Eigemann¹, Derek J. Smith³, Gregory J. Dick^{3,4}, Steven W. Wilhelm^{2*}

Harmful cyanobacteria are a global environmental problem, yet we lack actionable understanding of toxigenic versus nontoxigenic strain ecology and toxin production. We performed a large-scale meta-analysis including 103 papers and used it to develop a mechanistic, agent-based model of *Microcystis* growth and microcystin production. Simulations for Lake Erie suggest that the observed toxigenic-to-nontoxigenic strain succession during the 2014 Toledo drinking water crisis was controlled by different cellular oxidative stress mitigation strategies (protection by microcystin versus degradation by enzymes) and the different susceptibility of those mechanisms to nitrogen limitation. This model, as well as a simpler empirical one, predicts that the planned phosphorus load reduction will lower biomass but make nitrogen and light more available, which will increase toxin production, favor toxigenic cells, and increase toxin concentrations.

Harmful cyanobacteria and their toxins constitute one of the most important global environmental challenges faced by humanity, which is expected to get worse in a warmer climate (1, 2). The problem is exemplified by *Microcystis*, which can produce the potent hepatotoxin microcystin (MC), a class of cyclic nonribosomal peptides originally known as “fast death factor” that has already disrupted the drinking water supplies of Toledo, Ohio on Lake Erie and those of other cities (3).

In fresh waters, phytoplankton growth is often limited by the availability of phosphorous (P), and that concept has been applied in mathematical models and used to control bulk biomass—i.e., eutrophication—in many systems (4). It is also the basis for a costly binational agreement aimed at controlling toxic cyanobacteria in Lake Erie using a 40% P load reduction (5). However, this simple model does not address or explain the ecology of toxigenic versus nontoxigenic strains or the production of toxins, where nitrogen (N), temperature, and reactive oxygen species [e.g., hydrogen peroxide (H₂O₂)] are important factors (6–10). Advances in our understanding and management of cyanobacteria necessitate the development of new conceptual and quantitative models that incorporate relevant mechanisms.

The biology of *Microcystis*, including toxin production, has been extensively investigated in the laboratory, and a natural first step in the development of a next-generation model is to summarize and synthesize this information.

We performed a broad literature meta-analysis, including 103 papers published from 1958 and totaling 708 experiments (i.e., cultures, all cataloged and discussed individually in the supplementary materials). Experiments were conducted with 67 strains using various methods. Consequently, the database is heterogeneous, but some consistent and ecologically relevant patterns emerge (Fig. 1; model results discussed subsequently). Across 20 experiments, the optimum T for MC production is not 6.3°C, it is 6.3°C less than that for growth (Fig. 1A). As expected from the chemical formula of MC, which includes ~10 N atoms per molecule, lower N availability reduces MC content (Fig. 1B). The observed MC content can be higher or lower at increased light, which is also affected by binding to proteins (Fig. 1, C and F) (9, 11). These patterns show that the catalog of observations is a useful resource, even without model analysis.

Building on this large catalog of observations and existing cyanobacteria models (12) and following a pattern-oriented modeling approach (13), we developed a dynamic, mechanistic, and molecular-level model of *Microcystis* growth and toxin production. The agent-based model (ABM) simulates individual cells (14), with explicit representation of select representative genes with corresponding transcripts, enzymes, and metabolite pools (Fig. 2 shows a subset of the model). For example, *mcyD* is used as a proxy for all 10 genes in the MC synthesis cluster. The model includes a single gene, *t2prx*, as a representative of all H₂O₂-degrading enzymes [e.g., *katG* and *trxA* (10, 15)]. GLU and G3P represent labile N and C pools.

We repeated each experiment in the database in silico using the model. The ability of the model to reproduce observations is quantified using a pattern-oriented approach, where we identify patterns in the observations and compare them with the model (12) (supple-

mentary materials). In total, there are 897 patterns, and the model reproduces 87% of them. Mechanistic modeling thus provides a natural and intuitive way to summarize and interpret observations for *Microcystis*, as has been found for other organisms (12, 16).

The model can reproduce the relatively simple temperature optima, but also the more complex effect of N on MC content (Fig. 1B). It also predicts the decrease in free or measurable MC content at higher light intensities, which is the result of increased MC binding to proteins (9, 11). In some cases, the model proposes mechanisms underlying previously unexplained observed patterns, like the transient increase in MC content upon light downshift (Fig. 1D). In the model, this pattern is related to the dynamics of G3P and GLU, which are the limiting substrates for biomass synthesis and MC synthesis, respectively, in this experiment (fig. S109). When the light intensity decreases abruptly, photosynthesis and G3P content drop rapidly, and biomass decreases. However, N assimilation continues, and the biomass-based GLU content increases. Consequently, biomass-based MC synthesis increases. The *mcyD* gene is down-regulated rapidly upon light-downshift, but it takes some time for the enzyme level to respond. Once this occurs, the MC synthesis and content also decrease.

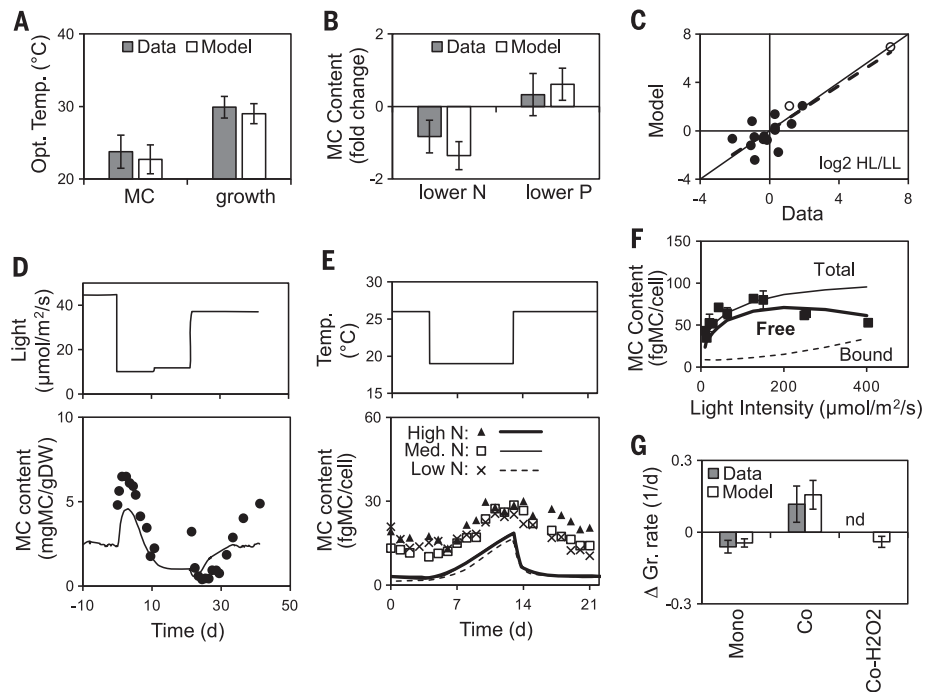
For some experiments, there can be substantial differences between observations and model predictions (Fig. 1E). This can be partially attributed to the constraint of calibrating the model with one parameter set (for each strain) to multiple datasets. There are experiments from 28 papers for this strain in the database. However, the main purpose of the model application to the database is to test its structure, i.e., mechanisms; differences in magnitude are less relevant than patterns because they can be calibrated for any field application of the model. In this example (Fig. 1E), the main observed pattern, the increase in MC content upon temperature decrease and vice versa, is reproduced by the model.

The key to understanding the differential ecology of toxigenic and nontoxigenic strains lies in the biological role of MC. There is increasing evidence that MC binds to enzymes and protects them from damage by reactive oxygen species, such as H₂O₂ (7, 9). Experiments with toxigenic wild-type and nontoxigenic *ΔmcyB* mutant cells show that, when H₂O₂ is added at environmentally relevant concentrations, the MC producer is less vulnerable than the non-MC-producing mutant (7) (Fig. 3). By contrast, when H₂O₂ is added at very high concentrations—levels corresponding to algicide or cyanocide treatment—the MC producer is more vulnerable (15). These observed patterns are relevant to the strain-level ecology and test the structural realism of the model.

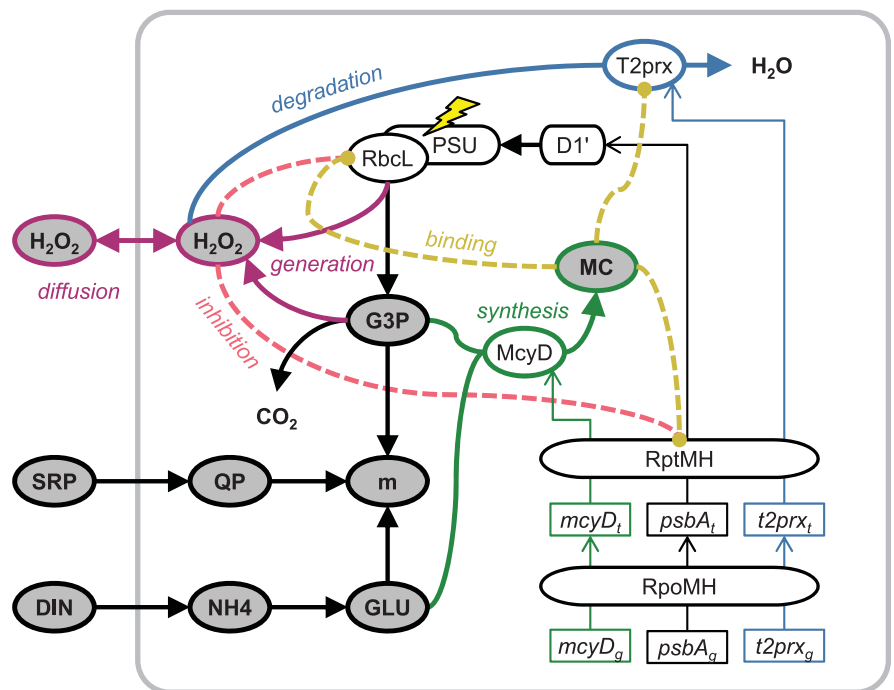
¹Water Quality Engineering, Technical University of Berlin, Berlin, Germany. ²Department of Microbiology, University of Tennessee, Knoxville, TN, USA. ³Department of Earth and Environmental Sciences, University of Michigan, Ann Arbor, MI, USA. ⁴Cooperative Institute for Great Lakes Research, University of Michigan, Ann Arbor, MI, USA.
*Corresponding author. Email: ferdi.hellweger@tu-berlin.de (F.L.H.); wilhelm@utk.edu (S.W.W.)

Fig. 1. Patterns of toxin production in *Microcystis* and comparison with model.

(A) Temperature optima for MC production and growth ($n = 20$); error bars are 95% CIs. (B) MC content under lower N ($n = 41$) and P ($n = 24$) relative to control; values are \log_2 ratios. (C) MC content (solid symbols) or *mcy* transcripts (open symbols) at high relative to low light (HL/LL) ($n = 16$); values are \log_2 ratios. Diagonal solid line is 1:1 (indicating perfect model-data agreement), and the dashed line is linear regression; $R^2 = 0.77$. (D and E) Transient response of MC content to changes in light (D) and temperature (E) in continuous culture. Data are from (8, 27). (F) MC content versus light. Data are from (11). Symbols are data, and lines are models in (D) to (F). (G) Relative fitness of toxigenic and nontoxigenic strains in mono- and coculture under various light, temperature, and nutrient conditions ($n = 13$). Growth rate difference (Δ Gr. rate) indicates the toxigenic – nontoxigenic growth rate. Co-H₂O₂ is a coculture simulation with the H₂O₂ damage turned off to illustrate that the advantage of the toxigenic strain in coculture is the result of interaction through H₂O₂. Data are from (18). nd, no data.

**Fig. 2. H₂O₂ generation, damage to enzymes and protection by MC, or degradation by T2prx in the model.**

Only select components and processes are shown; see supplementary materials for full model details. H₂O₂ is generated by photosynthesis and respiration, diffuses across the membrane, and inhibits enzymes, including PSURbcL and RptMH (ribosome). MC is synthesized from G3P and GLU and binds to and protects enzymes. T2prx (peroxiredoxin, used as a proxy for all H₂O₂ degradation enzymes) degrades H₂O₂.



The model includes generation of H₂O₂, damage to enzymes by H₂O₂, and two H₂O₂-management systems, including protection by MC and degradation by T2prx (which represents all H₂O₂-degrading enzymes) (Fig. 2), and it reproduces the observations (Fig. 3). The pattern at low-H₂O₂ levels can simply be attributed to protection by MC. The pattern at high-H₂O₂ levels is more complex. In the model, before the H₂O₂ addition, the wild-type strain relies on the MC system for H₂O₂

management and has the T2prx system down-regulated. When hit with H₂O₂, the MC system is overwhelmed. The cells express *t2prx*, but by this time, the ribosomes are damaged and do not recover. The mutant, however, has the T2prx system active before H₂O₂ addition and rapidly degrades the H₂O₂ and recovers. These are the mechanisms underlying the pattern in the model, which is consistent with the observed pattern. The model thus constitutes a

viable mechanistic explanation or hypothesis for the mechanisms responsible for the observed pattern.

In the high-H₂O₂ experiment, the toxigenic strain down-regulated H₂O₂-degrading enzymes under ambient conditions. This general strategy of protection against H₂O₂ by MC over degradation with enzymes may also be reflected in the gene repertoire of *Microcystis* strains—e.g., *katG* genes are less frequently found in toxigenic genotypes (10).

H_2O_2 readily diffuses across cell membranes, and the model predicts that degradation by the nontoxic strain leads to lower extracellular H_2O_2 levels, which also benefits the toxic strain—like the interaction between marine cyanobacteria and heterotrophic bacteria demonstrated previously (17). This interaction mechanism can explain observations where toxic strains outcompete nontoxic strains in coculture, despite equal or lower growth rate in monoculture (18, 19) (Fig. 1G).

The success of the model in reproducing *Microcystis* biology suggests that it may provide useful insights into ecology at the field scale. To test this, we simulate the water column around the Toledo drinking water intake during the 2014 growing season, when MC was detected in the drinking water (Fig. 4A). We use a simplified approach and simulate a completely mixed box [continuous stirred tank reactor (CSTR)] with dissolved inorganic

nitrogen (DIN) and soluble reactive phosphorus (SRP) input rates estimated from observed in situ DIN, SRP, and phycocyanin (PCN) concentrations and including estimates of photochemical H_2O_2 production (20) (details in section S3). The simulation includes toxic and nontoxic strains that differ only in their H_2O_2 management strategy—i.e., the toxic strain has *mcyD* and the nontoxic has *t2prx*—so any differences in their behavior can be directly attributed to these mechanisms. The parameters of the Lake Erie strains (same for toxic and nontoxic) were calibrated within the range of the laboratory strains, except that a lower H_2O_2 membrane permeability is needed, which may be associated with colony formation in the field.

The succession from toxic to nontoxic strains in the model is the result of differences in H_2O_2 management strategies that have different susceptibilities to N limitation

(fig. S11). In June and July, the DIN concentration is high, and the toxic strain can synthesize sufficient MC to protect its enzymes—it incurs less damage and outcompetes the nontoxic strain. In August and September, DIN is depleted, curtailing the production of MC by the toxic strain, which increases damage and lowers its growth rate. The *t2prx* system of the nontoxic strain is not affected by the lower DIN, and it outcompetes the toxic strain at that time.

Laboratory experiments show that N limitation results in lower MC levels (Fig. 1B) and that MC helps protect against H_2O_2 at ambient concentrations (Fig. 3) (7, 9). Together, these observations (and the model) suggest that toxic *Microcystis* is more vulnerable to H_2O_2 under N limitation, although that hypothesis has not yet been tested experimentally at environmental H_2O_2 levels.

Although our model does not consider all factors expected to affect strain-level ecology and toxin production (10, 21), it is based on mechanisms and reproduces the laboratory and field observations. It therefore represents a step forward in the mechanistic understanding of toxic cyanobacteria ecology and can inform lake management.

We used the model to evaluate load reduction scenarios, including 40% reduction in N, P, and both N and P (Fig. 4B). The largest biomass decrease is predicted for the N and P scenario, but all scenarios produce a decrease and none reach 40%, pointing to N, P, and light limitation. For the P-only reduction scenario, total *Microcystis* biomass decreases, but the increased N and light availability increase MC synthesis by the toxic strain (Fig. 1, B, C, D, and F), which lowers H_2O_2 damage and increases the toxic fraction. The toxic cells have more MC, and there are more of them. These two factors counteract the decrease in biomass and lead to increased MC concentration. When the effect of N and light on MC production is removed in the model, it predicts that MC concentration will decrease also for the P-only reduction scenario (Fig. 4B, part 1). Simulations where the P load reduction is focused earlier, when P is limiting (Fig. 4A, part 5) (22), are more effective at controlling biomass but will further increase MC concentrations through the same mechanisms as those for the even reduction (fig. S117). This pattern emerges in the relatively complex model, but the causal chain is simple and is predicted using a simple calculation or model that builds on mass balance and previous models and is parameterized directly from laboratory experiments (23, 24) (Fig. 4C and section S4).

In addition to changes in nutrient loads, global warming is expected to affect the lake (1–3, 25). For present loading, the model predicts cyanobacteria biomass increases and

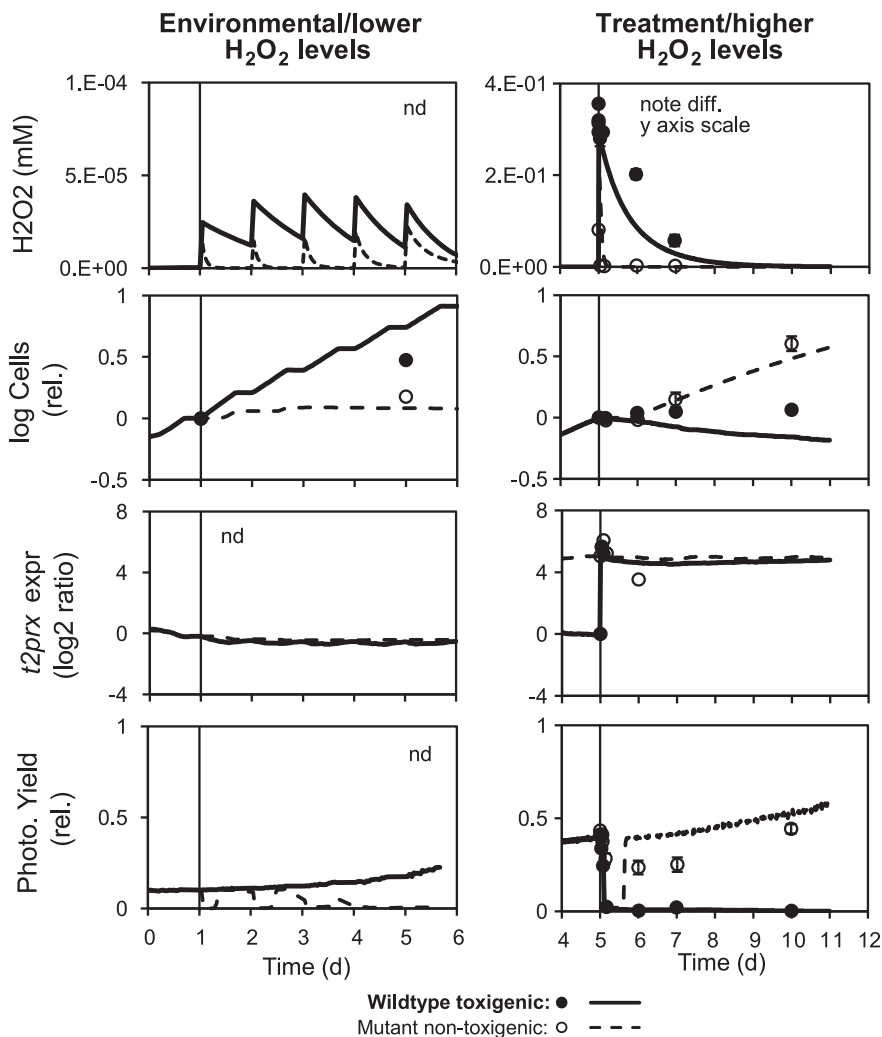


Fig. 3. H_2O_2 management and vulnerability of toxic and nontoxic strains. At environmental H_2O_2 concentrations (left), protection of enzymes by MC is advantageous. Data are from (7). At very high H_2O_2 concentrations, i.e., treatment levels (right), degradation is advantageous. Symbols are data, and lines are model. Data are from (15).

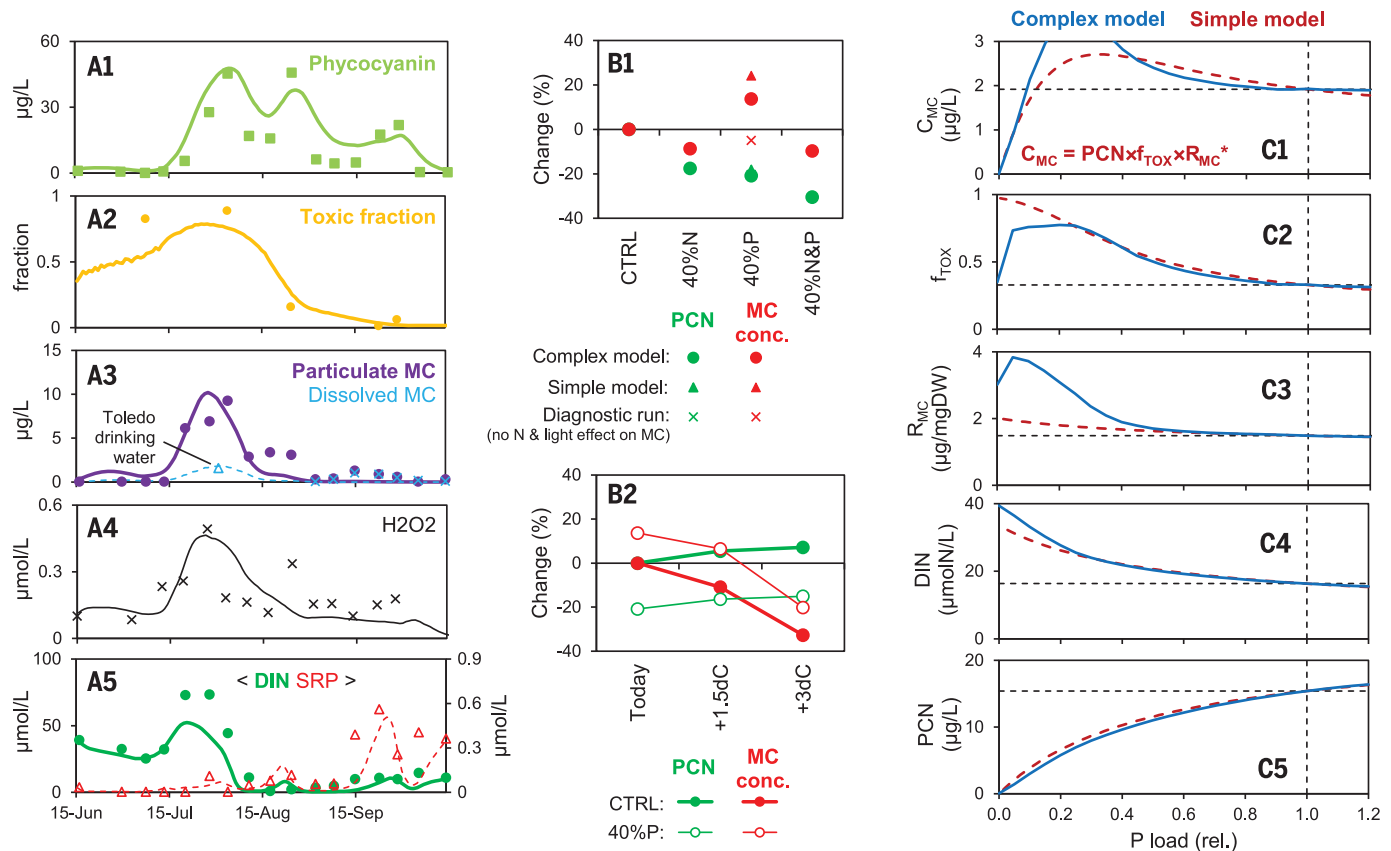


Fig. 4. Lake Erie simulation. Station W12 in 2014. **(A)** BaseCase model (lines) and data (symbols) versus time. From top to bottom, cyanobacteria biomass (PCN), toxigenic fraction, particulate and dissolved MC concentration (methanol-extractable fraction), H_2O_2 concentration, and nutrient concentrations are shown. See section S3 for additional results and discussion. Data are from this study and other sources (section S3). **(B)** Management and temperature scenarios. Shown are reductions in average PCN and observable MC relative to the current loading (CTRL) and temperature. Part 1 (top) is for present

temperature and shows all management scenarios, as well as results from the simple model and a diagnostic run to illustrate the effect of N and light. Part 2 (bottom) is for various temperature scenarios and shows current loading (CTRL) and 40% P-only reduction (40%P). **(C)** Response of full complex and a simpler model to reductions in P loading. From top to bottom, volume-based MC concentration (C_{MC}), toxigenic fraction (f_{TOX}), biomass-based MC content (R_{MC}), DIN concentration, and cyanobacteria biomass (PCN) are shown. The asterisk indicates units converted using 0.35 gC/gDW and 89 gC/gPCN, see table S4.

MC concentration decreases with rising temperature (Fig. 4B, part 2, CTRL). These results and observations of lower temperature optima for MC synthesis (Fig. 1A) suggest that toxin concentrations will not go up with the expected increase in biomass and brightens the otherwise bleak outlook for harmful cyanobacteria blooms. The model predicts that the temperature effect superimposes those of nutrient load reductions, and for the 40%P scenario, the net effect is a reduction in MC concentration for the higher temperature increase evaluated (Fig. 4B, part 2, 40%P). However, the decrease in MC concentration for this scenario is the result of the warmer temperature and not the P load reduction—i.e., the load reduction still increases the MC concentration relative to the warmer BaseCase scenario. These results suggest that P-only management is counterproductive for reducing MC concentration under all climate sce-

narios evaluated, and they support a dual N and P management strategy.

Our results suggest that future management efforts limited to P will increase relative availability of N and light, promote toxigenic strains, and increase toxin concentrations. This mechanism may be in part responsible for the presently observed resurgence of toxic cyanobacteria after historical P load reductions to Lake Erie and many other systems (26). Lake health is endangered by climate change and can be threatened by management actions that are well intended but based on an incomplete understanding of *Microcystis* biology and biochemistry. We may presently be witnessing the consequences of both threats

REFERENCES AND NOTES

1. H. W. Paerl, J. Huisman, *Science* **320**, 57–58 (2008).
2. S. C. Chapra et al., *Environ. Sci. Technol.* **51**, 8933–8943 (2017).

3. G. S. Bullerjahn et al., *Harmful Algae* **54**, 223–238 (2016).
4. D. W. Schindler, S. R. Carpenter, S. C. Chapra, R. E. Hecky, D. M. Orihel, *Environ. Sci. Technol.* **50**, 8923–8929 (2016).
5. United States Environmental Protection Agency, “U.S. Action Plan for Lake Erie” (2018); <https://www.epa.gov/glwqa/us-action-plan-lake-erie>.
6. C. J. Gobler et al., *Harmful Algae* **54**, 87–97 (2016).
7. C. Dziallas, H.-P. Grossart, *PLOS ONE* **6**, e25569 (2011).
8. R. M. Martin et al., *Front. Microbiol.* **11**, 601864 (2020).
9. Y. Zilliges et al., *PLOS ONE* **6**, e17615 (2011).
10. G. J. Dick et al., *Environ. Microbiol.* **23**, 7278–7313 (2021).
11. C. Wiedner et al., *Appl. Environ. Microbiol.* **69**, 1475–1481 (2003).
12. F. L. Hellweger et al., *Environ. Microbiol.* **18**, 2721–2731 (2016).
13. V. Grimm et al., *Science* **310**, 987–991 (2005).
14. F. L. Hellweger, R. J. Clegg, J. R. Clark, C. M. Plugge, J.-U. Kreft, *Nat. Rev. Microbiol.* **14**, 461–471 (2016).
15. J. M. Schuurmans et al., *Harmful Algae* **78**, 47–55 (2018).
16. D. N. Macklin et al., *Science* **369**, eaav3751 (2020).

17. J. J. Morris, Z. I. Johnson, M. J. Szul, M. Keller, E. R. Zinser, . *PLOS ONE* **6**, e16805 (2011).
18. L. Lei, C. Li, L. Peng, B.-P. Han, *Ecotoxicology* **24**, 1411–1418 (2015).
19. D. Schatz *et al.*, *Environ. Microbiol.* **7**, 798–805 (2005).
20. R. M. Cory *et al.*, *Front. Mar. Sci.* **4**, 377 (2017).
21. S. W. Wilhelm, G. S. Bullerjahn, R. M. L. McKay, *mBio* **11**, e00529-20 (2020).
22. R. P. Stumpf, T. T. Wynne, D. B. Baker, G. L. Fahnenstiel, *PLOS ONE* **7**, e42444 (2012).
23. B. M. Long, G. J. Jones, P. T. Orr, *Appl. Environ. Microbiol.* **67**, 278–283 (2001).
24. C. Vézic, J. Rapala, J. Vaitomaa, J. Seitsonen, K. Sivonen, *Microb. Ecol.* **43**, 443–454 (2002).
25. J. Trumpickas, B. J. Shuter, C. K. Minns, *J. Great Lakes Res.* **35**, 454–463 (2009).
26. H. W. Paerl *et al.*, *Hydrobiologia* **847**, 4359–4375 (2020).
27. H. Utkilen, N. Gjolme, *Appl. Environ. Microbiol.* **58**, 1321–1325 (1992).

28. F. L. Hellweger, fhellweger/Microcystis: version 1, version 1.0, Zenodo (2022); <https://doi.org/10.5281/zenodo.6383659>.

ACKNOWLEDGMENTS

Funding: This study was supported by National Oceanographic and Atmospheric Administration (NOAA) grant NA18NOS4780175 (to F.L.H. and S.W.W.). This is NOAA contribution no. 1018. This work was also supported by National Institute of Environmental Health Sciences grant IP01ES028939-01 (to S.W.W.), National Science Foundation grant OCE-1840715 (to S.W.W.), NOAA grant NA17NOS4780186 (to G.J.D.), and National Science Foundation grant OCE-1736629 (to G.J.D.). **Author contributions:** Conceptualization: F.L.H. Data curation: F.E. Formal analysis: F.L.H., R.M.M., D.J.S., and F. E. Funding acquisition: F.L.H., S.W.W., and G.J.D. Investigation: F.L.H., R.M.M., D.J.S., and F.E. Methodology: F.L.H. Project administration: F.L.H. and S.W.W. Resources: S.W.W. Software: F.L.H. Supervision: F.L.H. and G.J.D. Validation: F.L.H., R.M.M., D.J.S., and F.E. Visualization: F.L.H. Writing - original draft: F.L.H. Writing - review and editing: F.L.H., R.M.M., S.W.W., D.J.S., G.J.D.,

and F.E. **Competing interests:** The authors declare that they have no competing interests. **Data and materials availability:** The model code is available at Zenodo (28). The metagenomic reads used to calculate the fraction of toxic *Microcystis* are publicly available under NCBI BioProject no. PRJNA464361. **License information:** Copyright © 2022 the authors, some rights reserved; exclusive licensee American Association for the Advancement of Science. No claim to original US government works. <https://www.science.org/about/science-licenses-journal-article-reuse>

SUPPLEMENTARY MATERIALS

[science.org/doi/10.1126/science.abm6791](https://doi.org/10.1126/science.abm6791)
Supplementary Text
Figs. S1 to S131
Tables S1 to S37
References (29–180)
MDAR Reproducibility Checklist

Submitted 7 October 2021; accepted 25 March 2022
10.1126/science.abm6791



Models predict planned phosphorus load reduction will make Lake Erie more toxic

Ferdi L. Hellweger, Robbie M. Martin, Falk Eigemann, Derek J. Smith, Gregory J. Dick, and Steven W. Wilhelm

Science **376** (6596), . DOI: 10.1126/science.abm6791

Nutrient control must include nitrogen

Lake Erie receives water from important agricultural areas of Canada and the United States and is subject to high levels of nitrogen and phosphorus in runoff. These nutrients can lead to rapid growth of photosynthetic organisms, some of which produce toxins that harm aquatic animals and compromise drinking water. Recent efforts have focused on reducing phosphorus loading. With support from a large literature meta-analysis, Hellweger *et al.* developed an agent-based model of cyanobacterial metabolism to determine how toxin production changed under a range of nutrient and environmental conditions and defined the associated molecular mechanisms (see the Perspective by Ofi#eru and Picioreanu). They found that phosphorus reduction alone was potentially harmful, lowering total biomass but increasing toxin production. The proposed mechanism involves response to hydrogen peroxide stress and increased light transmission. —MAF

View the article online

<https://www.science.org/doi/10.1126/science.abm6791>

Permissions

<https://www.science.org/help/reprints-and-permissions>

Use of this article is subject to the [Terms of service](#)

Science (ISSN 1095-9203) is published by the American Association for the Advancement of Science, 1200 New York Avenue NW, Washington, DC 20005. The title *Science* is a registered trademark of AAAS.

Copyright © 2022 The Authors, some rights reserved; exclusive licensee American Association for the Advancement of Science. No claim to original U.S. Government Works